Advances in Science and Technology Research Journal

Advances in Science and Technology Research Journal, 2025, 19(5), 390–406
https://doi.org/10.12913/22998624/202212
ISSN 2299-8624, License CC-BY 4.0

Received: 2025.01.30
Accepted: 2025.03.15
Published: 2025.04.01

Determination of the criterion for the use of a toroidal mandrel during the mechanical bending of pipes with varying wall thicknesses

Zenon Grządziel[1*], Krzysztof Nozdrzykowski[1], Rafał Grzejda[2]

[1] Faculty of Marine Engineering, Maritime University of Szczecin, ul. Willowa 2, 71-560 Szczecin, Poland
[2] Faculty of Mechanical Engineering and Mechatronics, West Pomeranian University of Technology in Szczecin, ul. Piastów 19, 70-310 Szczecin, Poland
* Corresponding author's e-mail: z.grzadziel@pm.szczecin.pl

ABSTRACT

This paper presents the results of model tests related to the process of forming a pipeline arch by mechanical mandrel bending. The problems that occur during the pipeline manufacturing process and the methods and instrumentation used in forming the bent section of a pipeline, in particular the so-called mandrel bending, are presented. The main part of the paper consists of the results of model tests of stresses and deformations arising from the process of forming the arc of a mechanically bent pipeline using the proposed version of the mandrel with a torus-shaped forming part. These studies included an analysis of the effect of the pre-positioning of the mandrel on the values of deformations and stresses occurring in the cross-section of the bent pipe arch as a function of changes in the wall thickness and external diameter of the pipe and the bending radius. Based on the test results obtained, criteria were established enabling the selected pipe bending method to be used so that the resulting stresses and dimensions in the cross-sections of the bent pipe section are within the limits imposed by the normative recommendations. It was also shown that the criterion determining the efficiency of the bending process is the allowable recommended value of the ovalisation of the pipe cross-section.

Keywords: pipelines, mechanical mandrel bending, stress and strain modelling, cross-sectional geometry assessment.

INTRODUCTION

In numerous sectors of the economy, the transfer of a working energy medium (such as liquids or gases) takes place via industrial fittings. Such sectors include, for example, conventional power plants [1], gas pipelines [2] or waste incineration plants [3]. Industrial fittings are also indispensable in the automotive industry [4], aviation, aerospace and the wider marine industry and related units, including the shipbuilding industry [5, 6].

The pipeline plan is designed according to the technologist's guidelines. However, it is often adapted to the secondary structure (such as ceilings, beams, subsoil). For this reason, there are both straight and bent sections along the entire length of the pipeline. Industrial fittings are therefore assembled using straight and bent pipe sections and various types of fittings, couplings, reducers and flanges. Associated and measuring instrumentation such as valves, gate valves, orifices, dampers, expanders, pressure gauges, etc. are also installed along the length of the pipeline.

Depending on the intended use, the components that make up the pipelines are made of materials that ensure the required product quality, thus meeting the expectations of a range of industries as well as engineers, designers and customers [7, 8]. From the point of view of the effects of the manufacturing process of the various types of pipeline components, the process of manufacturing a bent pipeline section in particular deserves attention. During the bending process, there is an ovalisation of the cross-section with a simultaneous change in the thickness of the pipe wall at its circumference [9–11]. The bending process is also

accompanied by an increase in the reduced stresses occurring in the bent pipe, sometimes resulting in the need to apply an appropriate heat treatment (annealing), after the product forming process has been completed. Changes in cross-sections interfere with the flow of the working medium and make cleaning and maintenance, necessary to maintain the serviceability of the pipeline, more difficult. These changes also contribute to a reduction in the strength of the bent component in the tension zone, where the phenomenon of pipe wall thinning occurs [12]. In addition, the greater the ovalisation, the greater the error in the calculation of the stress distribution along the pipeline route. In a perfectly circular cross-section, there is a different pressure distribution than in a component with an elliptical outline. Hence, bend-shaped pipeline sections are subject to assessment of their dimensional shape performance, according to the applicable standards. For the energy industry, for example, the applicable standard in this respect is EN 13480 [13]. It defines the permissible corrugation of the compression layer, the maximum permissible ovalisation and the minimum wall thickness in the tension layer.

Depending on the type of technology used, there are several basic bending methods used in industrial settings to suit a particular type of pipe. In general, however, two types of pipe bending technology can be distinguished: cold [14–16] and hot [17–19]. One of the more modern and improved technologies for cold mechanical pipe bending is the so-called mandrel bending [20]. This method is ideal for shaping pipes with a very small bending radius. During bending, a so-called mandrel is inserted into the centre of the pipe being shaped. Depending on the type of pipe to be bent and the bending radius, the pipe is filled using straight, ball or segment mandrels [12, 21]. The diameters of the segments are smaller than the inner diameter of the pipe, which allows the pipe to be stiffened from the inside and the mandrel to be removed freely after the bending process.

In addition to the previously mentioned solutions for mandrels used in pipe bending, there are also known special design solutions for mandrels contained in the description of patent Pat.203569 [22] and included in the description of utility model Ru.058109 [23]. The use of a mandrel in the pipe (or profile) bending process prevents distortion, corrugation of the bent curve or its flattening and collapse. Greater control over the desired ovalisation of the pipes can be achieved. The use of mandrel bending technology also eliminates the tendency for the material to return to its original shape.

Mandrel bending is the technique most commonly used to process pipes with small bending radii (when the bending radius has a dimension corresponding to 3 times the pipe's outside diameter). The mandrel regulates the plastic flow of the material in the working area to maintain the required bending radius of thin-walled pipes and avoid undesirable deformation of the bent pipe section [24]. A mandrel is necessary if the diameter of the pipe is at least 20 times its thickness. Otherwise bending of pipes using a mandrel is not necessary, as the forces in the working area are not sufficient to cause the pipe to undulate.

There is no scientific justification for the recommended mandrel positioning in the available reference materials. The guidelines given are either estimates or recommend a trial and error method to determine the mandrel positioning. Such recommendations for users are given by most companies producing various types of mandrel bending machines for pipes as well as their authorised representatives. Shaping of a pipe section using this method can be carried out up to a bending angle of 90°. At larger bending angles, difficulties are encountered when removing the mandrel from the pipe.

The observations made during the pipeline process improvement work prompted research to determine the effect of mandrel positioning on strain and stress values and the geometric condition of a mandrel-bent pipeline section.

The values of stresses and strains in a bent pipe can be determined by analytical methods [25], but the finite element method (FEM) is most commonly used for this purpose [26–31]. However, when modelling thin-walled pipes, similar modelling techniques can be used as for other thin-walled systems [32–34]. Wang et al. [35] modelled the bending of thin-walled pipes using a diameter-adjustable mandrel constructed from core ball segments. Modelling of pipe bending using a mandrel similar in design was also presented earlier by Cheng et al. [36] and Jiang et al. [37]. The results of a study of neutral axis displacement in rotary drawing pipe bending processes using a mandrel were presented by Engel and Hassan [38]. A chain-link mandrel for rotary pipe bending was used in the modelling described by Salem et al. [39]. Razali et al. [40] performed an implicit elastoplastic finite element analysis of pipe bending with a focus on predicting springback.

With the above in mind, FEM was also used in the development of this article. The calculations were carried out using Midas NFX 2021 [41, 42]. The most important conclusion from the work carried out is that the criterion determining the efficiency of the bending process is the permissible recommended value of the ovalisation of the pipe cross-section. The paper also shows that the use of a dedicated bending process method for the imposed geometric dimensions of the pipe and radius will allow the ovalisation of the cross-section not to exceed its permissible value. The results of the analyses carried out allow the selection of a pipeline bending method depending on the pipe cross-sectional dimensions and the bending radius. It was finally shown that the use of the proposed toroidal mandrel in the mechanical bending process can lead to satisfactory results of the bending process.

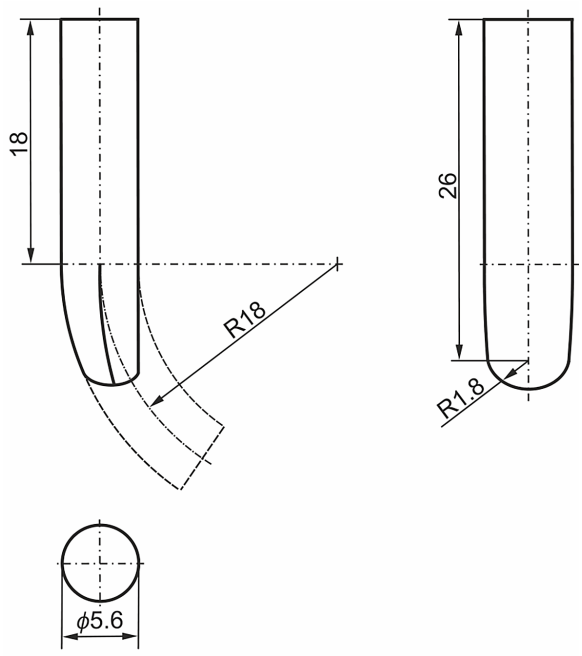

Figure 1. Shape of the mandrel used in simulation studies

METHODS

Simulation studies of deformations and stresses were carried out for the case of bending a pipe without a mandrel and with a mandrel by varying the pipe wall thickness. The calculations were carried out by varying the dimensions of the cross-section of the bent pipe (outer diameter D_o, inner diameter D_i and the resulting thickness g as well as the bending radius R) and the value of the mandrel displacement in relation to the bending axis. A mandrel with an extended end corresponding to the shape of a torus was taken as the filler in each case. The dimensioned shape of the toroidal mandrel adopted in the simulation study is presented in Figure 1. In the case of using a mandrel, in addition to changing its diameter as dictated by a change in the thickness of the pipe wall, its output positioning relative to the forming segment's axis of rotation was changed. This positioning was determined by the transition point of the mandrel's cylindrical shape into the torus portion. The mandrel extension beyond the axis of rotation was treated as a positive displacement, denoted as x. Retreat of the mandrel in front of the axis of rotation was treated as a negative displacement. The adopted method of determining the positioning of the mandrel and its location during the implementation of the pipe bending process is illustrated in Figure 2.

The first tests included 90-degree bending of two types of pipe with the parameters given

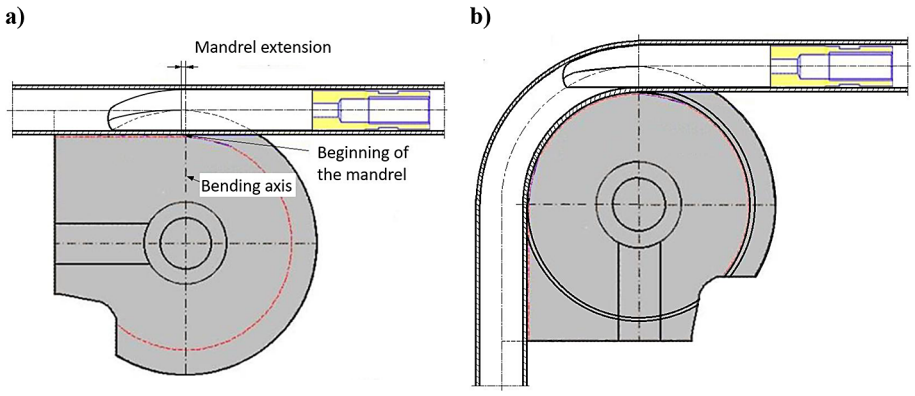

Figure 2. Location of the mandrel during the bending process: (a) determination of mandrel positioning, (b) positioning of the mandrel during the process

in Table 1. The dimensional changes of the pipe were checked in cross-sections defined by an angle α varying every 15 degrees (see Figure 3).

An elastic-plastic material model was used to represent the individual pipe types in the form of the bilinear characteristics shown in Figure 4. This characteristic is typical of stainless steel (such as 1.4571), for which the Young's modulus is 210 GPa, the yield strength is 210 MPa and the strengthening modulus is equal to 678 MPa. In contrast, the mandrel and rollers were modelled as rigid solids in the individual models.

Depending on the changes in the bending parameters (pipe dimensions, mandrel, bending radius), the number of finite elements adopted to model the components forming the tooling to be used in the technological process of mandrel bending of pipes was changed proportionally. Hexagonal-type elements were used to build the individual models. A model of the type A pipe bending process in the FEM convention is shown in Figure 5, while the finite element mesh parameters for this pipe case are summarised in Table 2. In addition to the finite elements given in Table 2, rigid-type elements were used in the model, with which the non-deformability of the rollers and mandrel was modelled. General contact elements [43, 44] were used between the pairs pipe-left roller, pipe-right roller and pipe-mandrel. The following contact element parameters were adopted:

- scaling factor of normal stiffness equal to 1,
- scaling factor of tangential stiffness equal to 0.1,
- coefficient of friction equal to 0.2.

An example of the distribution of contact elements in the adopted models is shown in Figure 6 (for comparison, see [45]). Each model was modelled as symmetrical with respect to the Z0X plane (see Figure 5). The following boundary conditions were applied to the models:

- right roller performed a preset rotation of 90° relative to an axis passing through the geometric centre of the roller and parallel to the Y axis, in a counterclockwise direction,
- left roller rotated about an axis passing through the geometrical centre of the roller and parallel to the Y axis, in a clockwise direction; the rotation was forced by the friction that occurred at the contact between the left roller and the bent pipe,
- mandrel was only allowed to move relative to the Z axis,
- bottom surface of the pipe was rigidly connected to the bottom surface of the right roller.

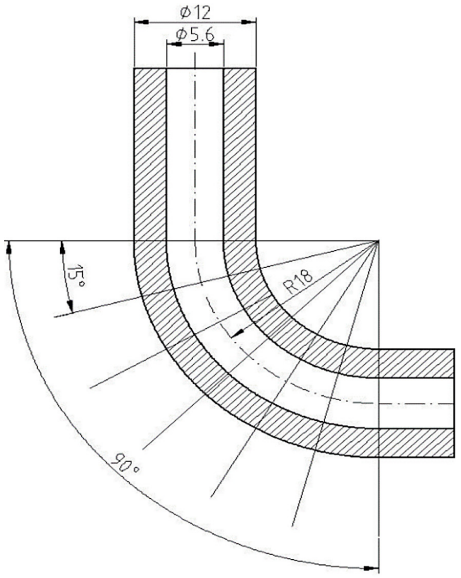

Figure 3. Angular location of individual cross-sections where variations in the diameter dimensions of the type A pipe bent at 90° were considered

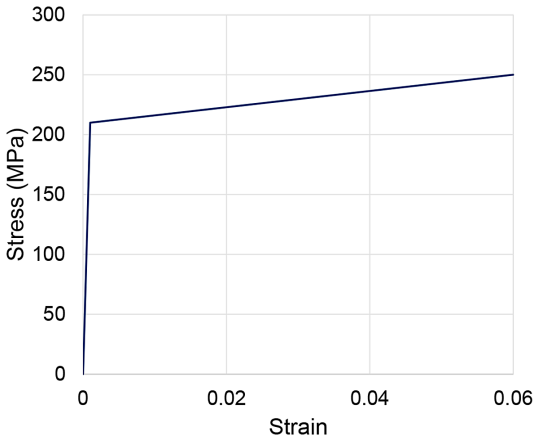

Figure 4. Characteristics of the elastic-plastic material used to model the individual pipes

Table 1. Parameters of pipe types tested

Pipe type	D_o (mm)	D_i (mm)	g (mm)	R (mm)
A	12.0	5.60	3.20	18.0
B	8.80	5.60	1.60	18.0

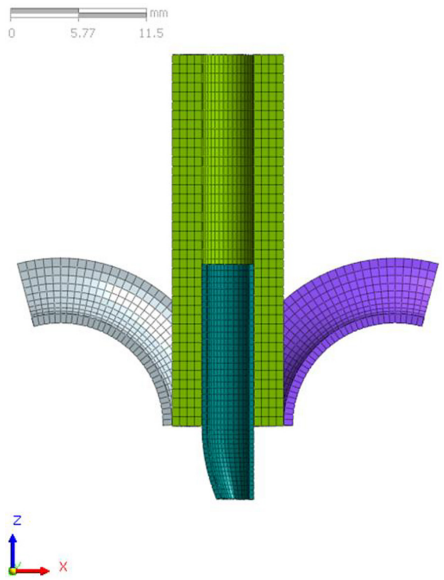

Figure 5. Angular location of individual cross-sections where variations in the diameter dimensions of the type A pipe bent at 90° were considered (light green – pipe, dark green – mandrel, grey – left roller, purple – right roller)

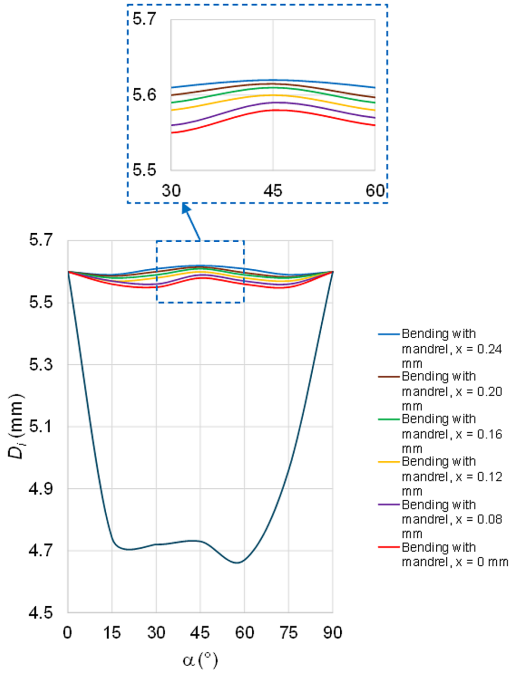

Figure 7. Variation of D_i diameter of the type A pipe as a function of the angle of the cross-section of the bent pipe

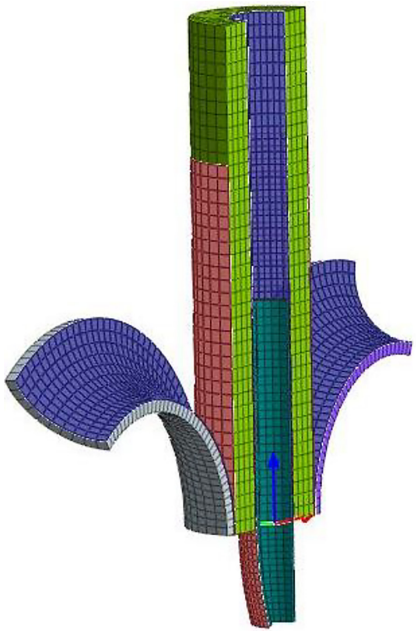

Figure 6. Distribution of contact elements in the adopted models (brown – master elements, dark blue – slave elements)

In the second part of the study to investigate the ovalisation phenomenon in more detail, pipe bending was also tested for other parameters than those described in Table 1. Thus, tests were conducted for a radius R, for which the following values were assumed: 16.4 mm, 36.0 mm, 84.0 mm and 96.0 mm, and for D_o equal to 32.0 mm and D_i equal to 28.8 mm.

RESULTS

The variation of D_i diameter of the type A pipe bent at 90° in individual cross-sections is shown in Table 3 and Figure 7. The angular position of the individual cross-sections is shown earlier in Figure 3. The variation of D_i diameter of the type A pipe as a function of the angle of the cross-section of the bent pipe and the mandrel extension is shown in Figure 8. The variation of D_i diameter

Table 2. Parameters of pipe types tested

Model part	Number of finite elements	Number of nodes
Pipe	3.312	4.465
Mandrel	630	1376
Left roller	760	878
Right roller	760	878

Table 3. Variation of D_i diameter of the type A pipe as a function of the angle of the cross-section of the bent pipe

α (°)	Bending without mandrel	Bending with mandrel at extension *x* (mm)					
		0	0.08	0.12	0.16	0.20	0.24
0	5.60	5.60	5.60	5.60	5.60	5.60	5.60
15	4.74	5.56	5.57	5.57	5.58	5.59	5.59
30	4.72	5.55	5.56	5.58	5.59	5.60	5.61
45	4.73	5.58	5.59	5.60	5.61	5.62	5.62
60	4.67	5.56	5.57	5.58	5.59	5.60	5.61
75	4.96	5.55	5.56	5.57	5.58	5.58	5.59
90	5.60	5.60	5.60	5.60	5.60	5.60	5.60

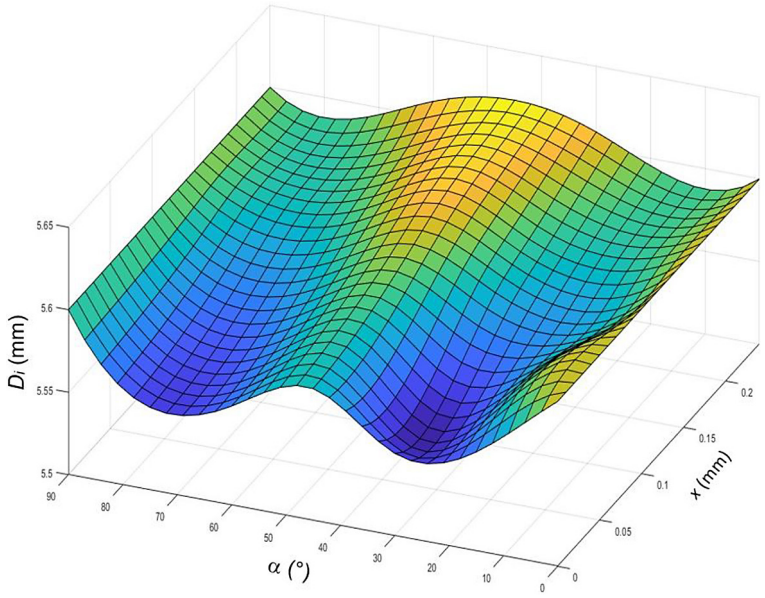

Figure 8. Variation of D_i diameter of the type A pipe as a function of the angle of the cross-section of the bent pipe

of the type B pipe bent at 90° in individual cross-sections is shown in Table 4 and Figure 9. The angular position of the individual cross-sections is shown earlier in Figure 3.

The variation of D_i diameter of the type B pipe as a function of the angle of the cross-section of the bent pipe and the mandrel extension is shown in Figure 10. An important parameter adopted in the assessment of the dimensions of the shaped pipe cross-section is ovalisation Δ *ow*, which according to PN-EN 13480-1 [46], taking the outer diameter of the pipe as the assessment criterion, should be calculated from the relationship:

$$\Delta ow = \frac{2(D_{o\,max} - D_{o\,min})}{D_{o\,max} + D_{o\,min}} \cdot 100\% \qquad (1)$$

where: $D_{o\,max}$ – maximum outer diameter, $D_{o\,min}$ – minimum outer diameter.

PN-EN 13480-1 [46] also gives an acceptable ovalisation value related to the bending radius R and the outer diameter D_o of the bent pipe, recommending the following relationship for its calculation:

$$\Delta ow = \frac{20}{\frac{R}{D_o}} = \frac{20}{m} \qquad (2)$$

where: m – dimensionless factor expressing the ratio between the bending radius R and the outer diameter D_o of the pipe.

Figure 11 shows a graph showing the variation of the acceptable ovalisation Δ *ow* as a function of the R/D_o quotient (i.e. the m factor).

Due to the observed slight variation in pipe diameters during mechanical bending with a mandrel depending on the angle of the location of the cross-section of the bent pipe curve, as well

Table 4. Variation of D_i diameter of the type B pipe as a function of the angle of the cross-section of the bent pipe

α (°)	Bending without mandrel	Bending with mandrel at extension *x* (mm)				
		0	0.06	0.12	0.18	0.24
0	5.60	5.60	5.60	5.60	5.60	5.60
15	4.97	5.55	5.55	5.55	5.56	5.56
30	4.97	5.57	5.58	5.58	5.59	5.60
45	5.03	5.59	5.60	5.61	5.63	5.64
60	4.94	5.58	5.59	5.61	5.63	5.64
75	5.01	5.56	5.57	5.58	5.60	5.61
90	5.60	5.60	5.60	5.60	5.60	5.60

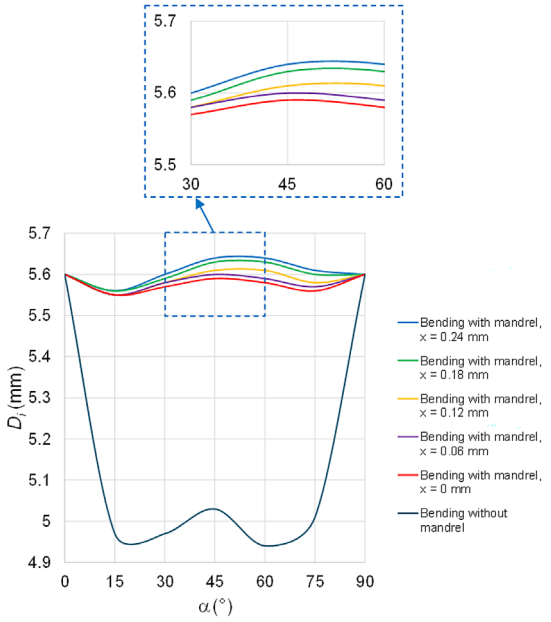

Figure 9. Variation of D_i diameter of the type B pipe as a function of the angle of the cross-section of the bent pipe

as taking into account normative recommendations, the subsequent modelling steps focused on assessing the ovalisation of the cross-section located only at an angle of 45°.

Taking into account that the degree of ovalisation is also influenced by the pipe wall thickness *g*, a second dimensionless coefficient *n* expressed as the quotient D_o/g was introduced, followed by a universal coefficient ψ combining *R*, D_o and *g*, described by the relation:

$$\psi = \frac{m}{n} \tag{3}$$

The maximum value of the pipe wall thickening g_{max} and the minimum value of the pipe wall thinning g_{min} were calculated based on relations of the form [47]:

$$g_{max} = g_{nom}\frac{m-0.25}{m-0.5} \tag{4}$$

$$g_{min} = g_{nom}\frac{m+0.25}{m+0.5} \tag{5}$$

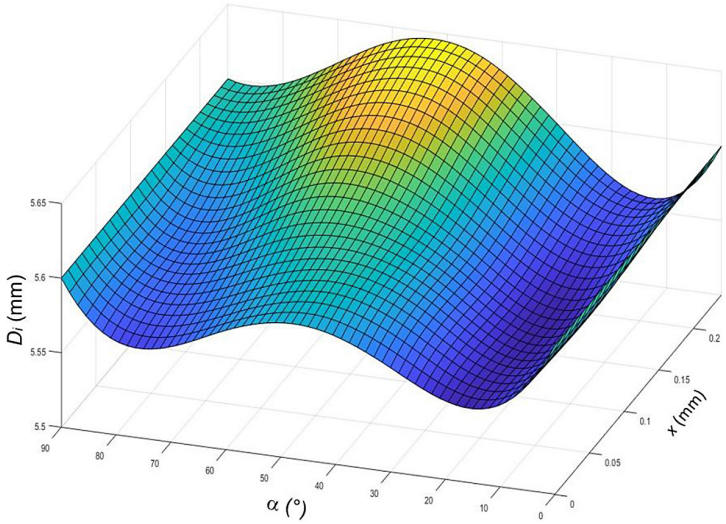

Figure 10. Variation of D_i diameter of the type B pipe as a function of the angle of the cross-section of the bent pipe and the mandrel extension

Whereby: if $\frac{D_o}{D_i} > 1.7$ then:

$$g_{nom} = \frac{D_o}{2}\left(1 - \sqrt{\frac{fz - p_c}{fz + p_c}}\right) \quad (6)$$

if $\frac{D_o}{D_i} \leq 1.7$ then:

$$g_{nom} = \frac{p_c D_o}{2fz + p_c} \quad (7)$$

where: g_{nom} – nominal pipe thickness (mm), f – design stress (MPa), z – section modulus for a pipe (mm^3), p_c – calculation pressure (MPa).

In order to carry out a final analysis of the bending process, calculations using FEM were carried out for various pipe parameters. Selected examples of the results obtained are shown in Tables 5 to 10, in which the extension of the mandrel x is specified as a percentage of its diameter. The acceptable value of the ovalisation of the pipe cross-section Δow was read from the graph presented in Figure 11.

Figure 12 shows an example of the variation of the pipe wall thickness in the longitudinal and transverse cross-sections for the selected case of simulation testing of bending a pipe with a mandrel as described in Table 6. An example of the deformed longitudinal and transverse cross-sections in the case of bending a pipe without a mandrel is shown in Figure 13.

As shown in Table 10, the bending of the thin-walled pipe using the proposed mandrel shape and small bending radius required a negative offset, i.e. the mandrel was moved back in front of the bending axis, to enable satisfactory

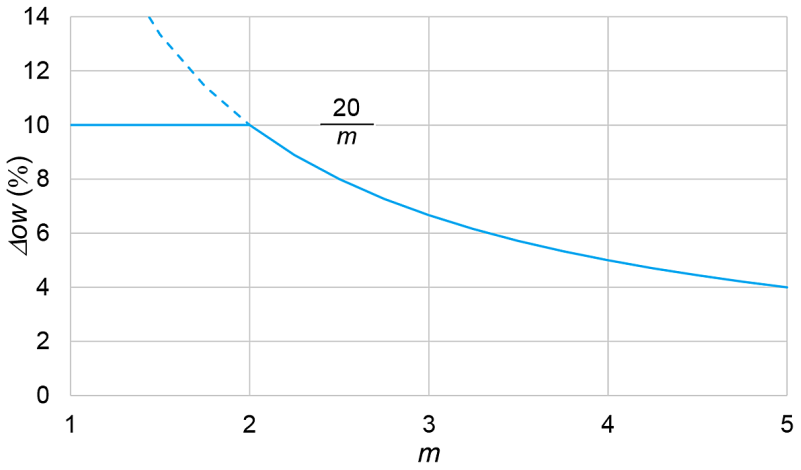

Figure 11. Course of variation of the acceptable ovalisation Δow as a function of the m factor (compiled from [46])

Table 5. The dimensions of the cross-section of the shaped pipe and the calculated values of the ovalisation of the internal and external diameters assuming: g_{nom} = 3.20 mm, D_i = 5.60 mm, D_o = 12.0 mm, R = 36.0 mm, n = 3.75; m = 3.00; ψ = 0.80; g_{max} = 3.57 mm; g_{min} = 2.97 mm and Δow = 6.7%

Parameter			Without mandrel	With mandrel	
				x = 0%	x = 10%
g_{nom}	Vertical plane	Max (mm)	3.48	3.27	3.27
		Min (mm)	2.95	2.86	2.86
	Horizontal plane (mm)		3.18	3.17	3.17
D_i	Vertical plane (mm)		5.29	5.58	5.59
	Horizontal plane (mm)		5.62	5.66	5.64
	Ovalisation (%)		6.05	1.42	0.89
D_o	Vertical plane (mm)		11.72	11.71	11.72
	Horizontal plane (mm)		11.98	12.00	11.98
	Ovalisation (%)		2.19	2.45	2.19

Table 6. The dimensions of the cross-section of the shaped pipe and the calculated values of the ovalisation of the internal and external diameters assuming: g_{nom} = 1.60 mm, D_i = 5.60 mm, D_o = 8.80 mm, R = 36.0 mm, n = 5.50; m = 4.09; ψ = 0.74; g_{max} = 1.71 mm; g_{min} = 1.51 mm and Δ ow = 4.9%

Parameter			Without mandrel	With mandrel	
				x = 0%	x = 10%
g_{nom}	Vertical plane	Max (mm)	1.75	1.65	1.65
		Min (mm)	1.50	1.56	1.56
	Horizontal plane (mm)		1.59	1.60	1.60
D_i	Vertical plane (mm)		5.40	5.16	5.14
	Horizontal plane (mm)		5.62	5.95	5.96
	Ovalisation (%)		3.99	14.2	14.8
D_o	Vertical plane (mm)		8.65	8.37	8.35
	Horizontal plane (mm)		8.80	9.15	9.16
	Ovalisation (%)		1.72	8.90	9.25

Table 7. The dimensions of the cross-section of the shaped pipe and the calculated values of the ovalisation of the internal and external diameters assuming: g_{nom} = 3.20 mm, D_i = 5.60 mm, D_o = 12.0 mm, R = 18.0 mm, n = 3.75; m = 1.50; ψ = 0.40; g_{max} = 4.00 mm; g_{min} = 2.80 mm and Δ ow = 10%

Parameter			Without mandrel	With mandrel	
				x = 0%	x = 5%
g_{nom}	Vertical plane	Max (mm)	3.79	3.41	3.35
		Min (mm)	2.72	2.44	2.49
	Horizontal plane (mm)		3.18	3.07	3.07
D_i	Vertical plane (mm)		4.73	5.58	5.62
	Horizontal plane (mm)		5.62	5.71	5.68
	Ovalisation (%)		17.2	2.30	1.06
D_o	Vertical plane (mm)		11.24	11.43	11.46
	Horizontal plane (mm)		11.98	11.85	11.82
	Ovalisation (%)		6.38	3.61	3.09

Table 8. The dimensions of the cross-section of the shaped pipe and the calculated values of the ovalisation of the internal and external diameters assuming: g_{nom} = 1.60 mm, D_i = 5.60 mm, D_o = 8.80 mm, R = 16.4 mm, n = 5.50; m = 1.86; ψ = 0.34; g_{max} = 1.89 mm; g_{min} = 1.43 mm and Δ ow = 10%

Parameter			Without mandrel	With mandrel	
				x = 0%	x = 5%
g_{nom}	Vertical plane	Max (mm)	1.83	1.70	1.68
		Min (mm)	1.42	1.28	1.27
	Horizontal plane (mm)		1.57	1.54	1.53
D_i	Vertical plane (mm)		5.03	5.59	5.64
	Horizontal plane (mm)		5.65	5.59	5.59
	Ovalisation (%)		11.6	0	-0.89
D_o	Vertical plane (mm)		8.28	8.57	8.59
	Horizontal plane (mm)		8.79	8.67	8.65
	Ovalisation (%)		5.98	1.16	0.70

results (maintaining the required wall thickness and ovalisation of the cross-section). An example of the pipe forming results obtained for this case are shown in Figure 14, which illustrates an image of the shaped longitudinal and transverse cross-section (at an angle of 45°) when bending a thin-walled pipe with the mandrel offset by 2% of the mandrel diameter in front of the bending axis.

Table 9. The dimensions of the cross-section of the shaped pipe and the calculated values of the ovalisation of the internal and external diameters assuming: g_{nom} = 1.60 mm, D_i = 28.8 mm, D_o = 32.0 mm, R = 96.0 mm, n = 20.0; m = 3.00; ψ = 0.15; g_{max} = 1.71 mm; g_{min} = 1.49 mm and Δ ow = 6.7%

Parameter			Without mandrel	With mandrel	
				X = 0%	X = 10%
G_{nom}	Vertical plane	Max (mm)	1.63	1.62	1.61
		Min (mm)	1.55	1.48	1.25
	Horizontal plane (mm)		1.60	1.60	1.56
D_i	Vertical plane (mm)		28.12	28.80	29.70
	Horizontal plane (mm)		28.75	28.80	28.58
	Ovalisation (%)		2.22	0	-3.84
D_o	Vertical plane (mm)		31.30	31.90	32.56
	Horizontal plane (mm)		31.95	32.00	31.70
	Ovalisation (%)		2.05	0.31	-2.68

Table 10. The dimensions of the cross-section of the shaped pipe and the calculated values of the ovalisation of the internal and external diameters assuming: g_{nom} = 1.60 mm, D_i = 28.8 mm, D_o = 32.0 mm, R = 84.0 mm, n = 20.0; m = 2.63; ψ = 0.13; g_{max} = 1.79 mm; g_{min} = 1.47 mm and Δ ow = 7.6%

Parameter			Without mandrel	With mandrel			
				x = -10%	x = -5%	x = -2%	x = 0%	x = 10%
G_{nom}	Vertical plane	Max (mm)	Corrugation	Corrugation	1.74	1.75	1.71	1.65
		Min (mm)			1.49	1.42	1.46	1.07
	Horizontal plane (mm)				1.59	1.60	1.59	1.53
D_i	Vertical plane (mm)				28.20	28.70	31.70	33.30
	Horizontal plane (mm)				28.72	28.80	28.82	28.94
	Ovalisation (%)				1.83	0.34	-9.52	-14.01
D_o	Vertical plane (mm)				31.39	31.87	34.87	36.02
	Horizontal plane (mm)				31.90	32.00	32.00	32.00
	Ovalisation (%)				1.61	0.40	-8.58	-11.82

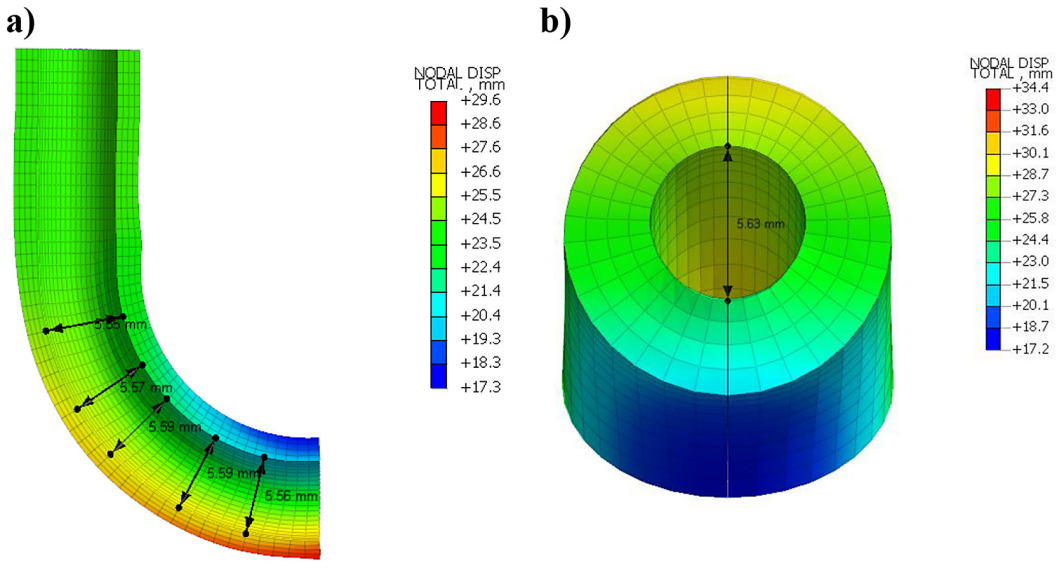

Figure 12. Example image of the variation of pipe wall thickness for a selected case of simulation testing of mandrel pipe bending described in Table 6: (a) in longitudinal cross-section, (b) in transverse cross-sections

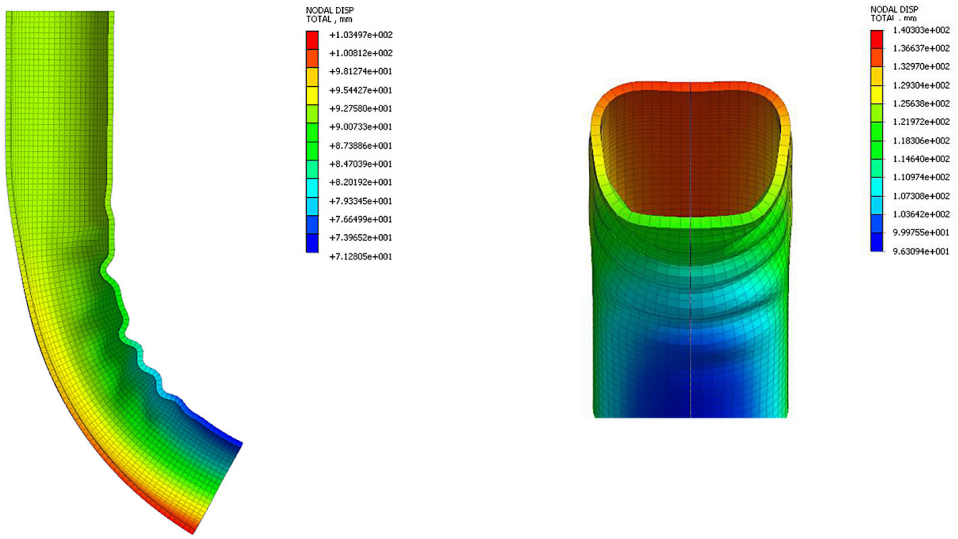

Figure 13. Example of deformed longitudinal and transverse cross-sections in the case of bending a thin-walled pipe without a mandrel

However, too much retraction of the mandrel results in undesirable corrugation of the inner wall of the pipe especially at the initial stage of 90° bending (see Figure 15). The fabricated sections of the pipe bent at 45° when the mandrel was moved significantly (5% of the mandrel diameter) in front of the bending axis and when the mandrel was moved slightly (2% of the mandrel diameter) in front of the bending axis are shown in Figures 16a and 16b, respectively. The pipes shown in Figure 16 were made on a bending machine of our own design.

The technological process of pipe bending is accompanied by changes in stress in addition to permanent deformation. An increase in stress above the permissible value results in the possibility of wall cracking in the bent pipe section. Therefore, the results of the deformation tests were supplemented in each case with stress analyses of the pipe bending process. The stress analysis additionally took into account the fact that the pipe section formed by mechanical bending is subjected to operating pressure during operation. The stresses in the longitudinal and transverse cross-sections were analysed for the case of pipe bending without and with a mandrel, and without and with working pressure, assuming the values p_c = 6.5 MPa and f = 103.3 MPa.

Table 11 shows the values of the maximum stresses σ_{yy} in the cross-section located at 45° for a pipe bent at 90°. The values of these stresses in graphical form are shown in Figure 17. Table 12 shows the values of the reduced stresses σ_{red} according to the Huber - von Mises - Hencky yield

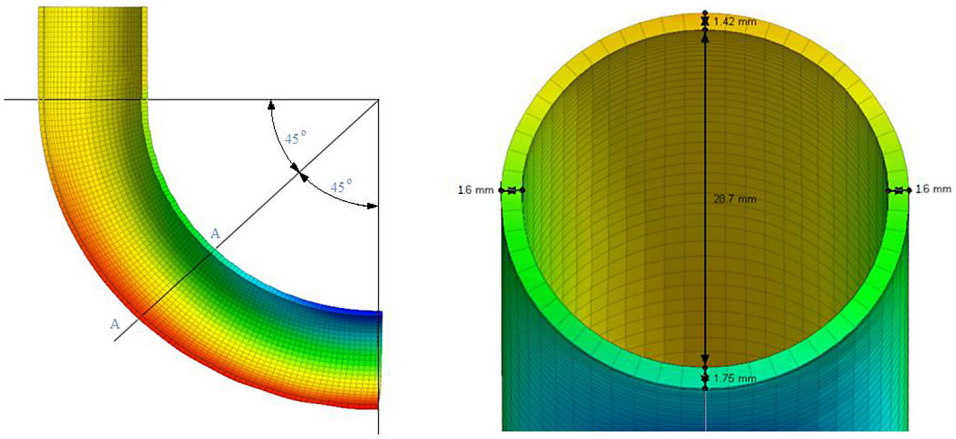

Figure 14. Image of the shaped longitudinal and transverse cross-section (at 45°) when bending a thin-walled pipe with the mandrel offset by 2% of the mandrel diameter in front of the bending axis

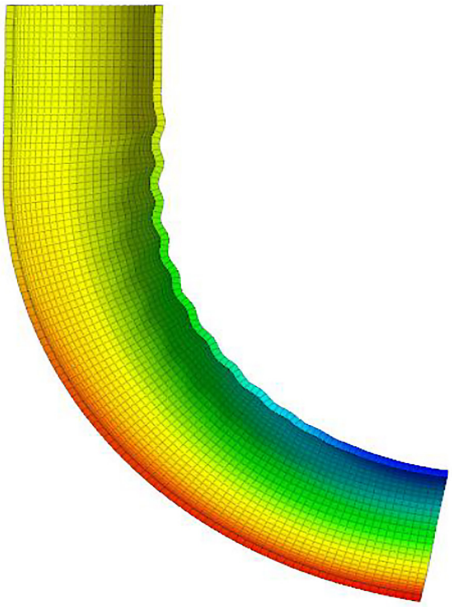

Figure 15. Image of the deformed longitudinal cross-section when bending a thin-walled pipe using the proposed mandrel shape, which was shifted significantly in front of the bending axis

criterion [29] in the cross-section located at 45° for a pipe bent at 90°. The values of these stresses in graphical form are shown in Figure 18.

DISCUSSION

In the deformation simulation studies, most of the results showed a typical variation in longitudinal and transverse cross-sections resulting from the bending process, manifested by a thinning of the pipe wall thickness at the outer surface in tension and a thickening of the pipe wall at the inner surface in compression, as illustrated, for example, in Figure 12. However, the resulting ovalisation of the pipe cross-section is within the permissible limits recommended by the standards. The mandrel bending process is accompanied by the characteristic formation of a notch, on the inner curve of the pipe at the end of the bend, suggesting the need for a smoothing device. The reduction of the ψ coefficient value below 0.20 that characterises thin-walled pipes and the absence of a mandrel results in deformations of the bent pipe arch that make it virtually impossible to determine its transverse dimensions (Figure 13). The use of a mandrel makes it possible to obtain a satisfactory cross-sectional shape of the pipe even if the value of the ψ coefficient decreases to 0.11. A decrease in the value of the ψ coefficient below 0.10 requires that bending be carried out with a ball mandrel in order to obtain the geometrical parameters of the shaped pipe required by the standards. The results of the analyses carried out made it possible to draw up the graph presented in Figure 19 showing the effect of the n factor on the change in the value of ψ, taking into account the recommended bending method and the permissible ovalisation Δow value. It consequently enables the selection of a bending method that, from the point of view of the recommended ovalisation, will ensure that the required effects of the pipe shaping process can be achieved, depending on the geometrical dimensions of the

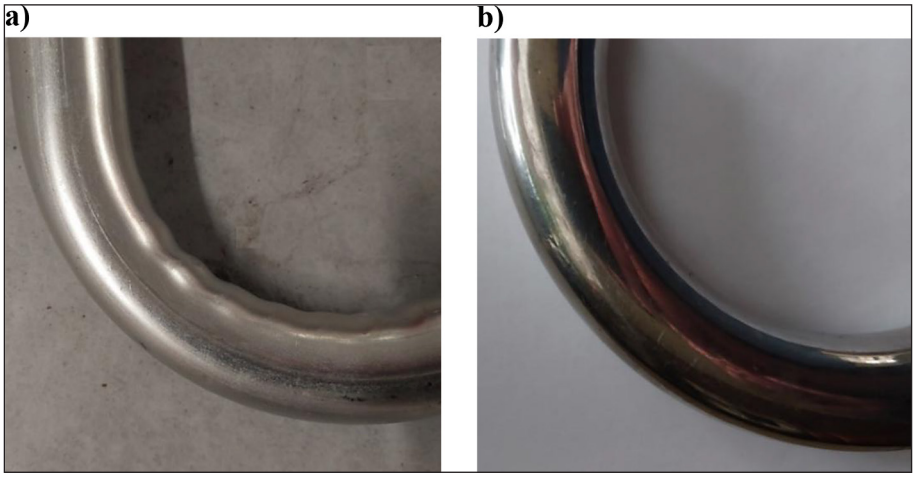

Figure 16. Executed sections of pipe bent at 45°: (a) where the mandrel is moved significantly (5% of the mandrel diameter) in front of the bending axis, (b) where the mandrel is moved slightly (2% of the mandrel diameter) in front of the bending axis

Table 11. Values of the maximum stresses σ_{rr} in the cross-section located at 45° for 90° bending of the type A pipe

Pipe wall thickness	Dimension *r* (mm) (see Figure 16)	Maximum stresses σ_{rr} (MPa)					
		Straight pipe	Pipe after bending without mandrel and without pressure	Pipe after ideal bending under pressure	Pipe after bending with mandrel and without pressure	Pipe after bending without mandrel and under pressure	Pipe after bending with mandrel and under pressure
Thinning of the pipe wall	0	36.2	96.5	29.1	100	58.1	52.8
	0.8	41.6	77.9	34.6	80.7	53.4	56.1
	1.6	50.9	24.1	44.6	31.9	49.7	62.9
	2.4	67.1	-73.8	61.6	-49.3	49.2	76.5
	3.2	94.7	-163	89.7	-138	51.0	99.0
–	4.0	–					
	4.8						
	5.6						
	6.4						
	7.2						
	8.0						
Thickening of the pipe wall	8.8	94.7	17.9	110	-92.7	45.4	89.7
	9.6	67.1	-46.5	75.3	-76.1	41.7	69.1
	10.4	50.9	10.7	60.2	8.30	43.9	56.5
	11.2	41.6	45.3	50.4	64.1	45.7	49.2
	12.0	36.2	49.1	43.9	92.1	46.4	44.5

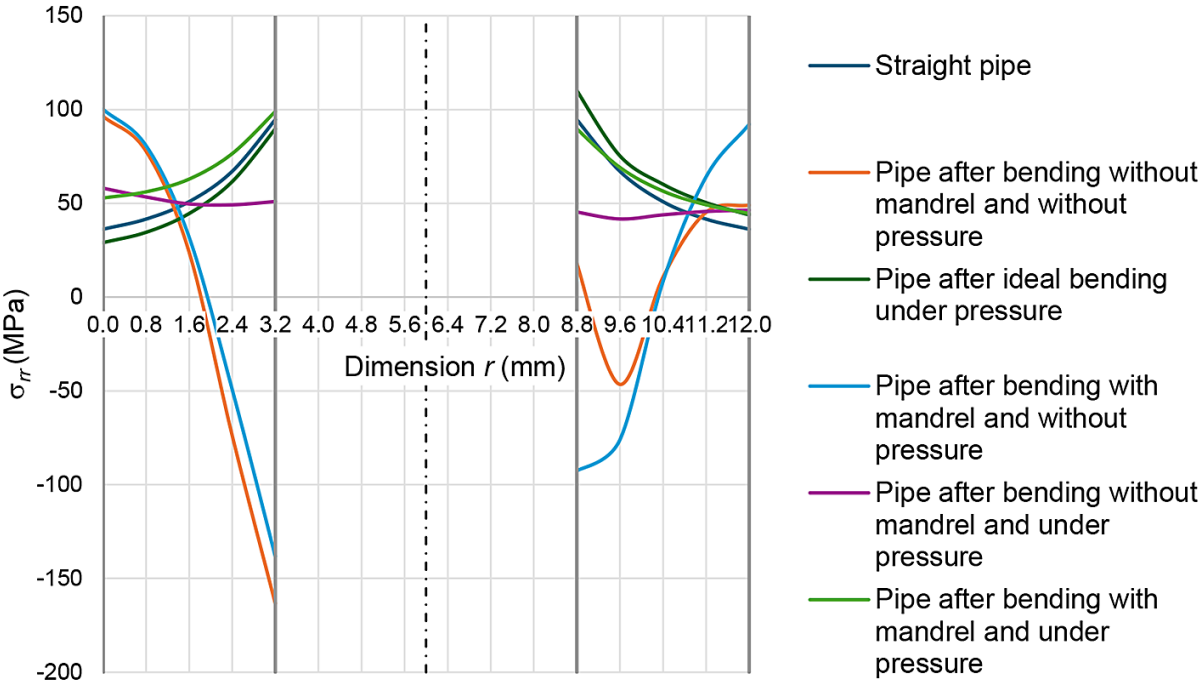

Figure 17. Values of the maximum stresses σ_{rr} in the cross-section at 45° for 90° bending of the type A pipe

pipe and the bending radius. The results of the study also showed that special care must be taken when bending using the proposed mandrel shape for thin-walled pipes and at small bending radii. It is important in these cases to have proper (skilful) positioning of the mandrel with respect to the bending axis, requiring a mandrel retraction (negative displacement), which was estimated to be a value

Table 12. Values of the reduced stresses σ_{red} in the cross-section located at 45° for 90° bending of the type A pipe

Pipe wall thickness	Dimension *r* (mm) (see Figure 17)	Maximum stresses σ_{red} (MPa)					
		Straight pipe	Pipe after bending without mandrel and without pressure	Pipe after ideal bending under pressure	Pipe after bending with mandrel and without pressure	Pipe after bending without mandrel and under pressure	Pipe after bending with mandrel and under pressure
Thinning of the pipe wall	0	32.4	131	25.6	43.7	54.7	47.2
	0.8	41.5	126	34.9	54.7	54.0	54.7
	1.6	57.9	99.6	51.5	35.1	62.2	69.7
	2.4	86.5	57.8	80.9	10.0	78.7	96.7
	3.2	132	267	128	26.1	93.1	136
–	4.0	–					
	4.8						
	5.6						
	6.4						
	7.2						
	8.0						
Thickening of the pipe wall	8,8	132	183	127	280	65.6	126
	9,6	86.5	145	77.6	77.3	57.0	90.6
	10,4	57.9	32.1	61.9	98.8	53.5	64.5
	11,2	41.5	70.2	48.0	109	46.0	48.8
	12,0	32.4	117	38.6	100	45.1	40.7

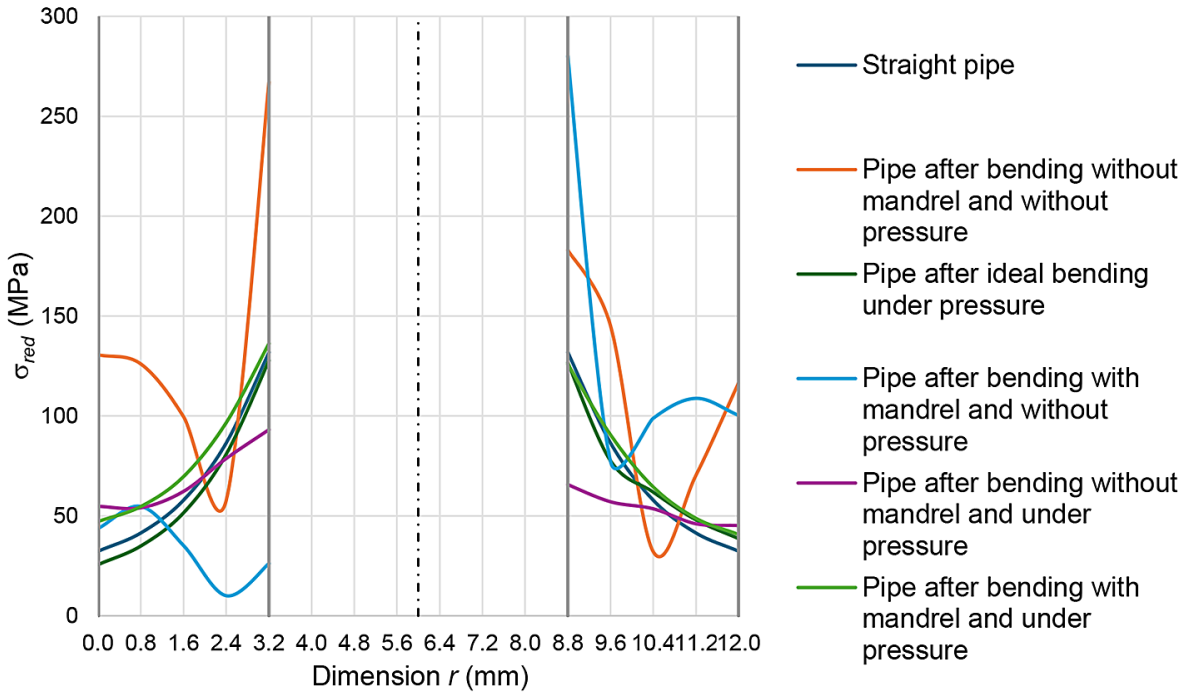

Figure 18. Values of the reduced stresses σ_{red} in the cross-section at 45° for 90° bending of the type A pipe

corresponding to 2% of the mandrel diameter, to enable satisfactory results of the pipe bending process. Analysis of the stresses accompanying the bending process showed considerable variability, with stress values not exceeding the values permitted for the material adopted in the study, which is the material used for the piping components of a marine power plant supply system.

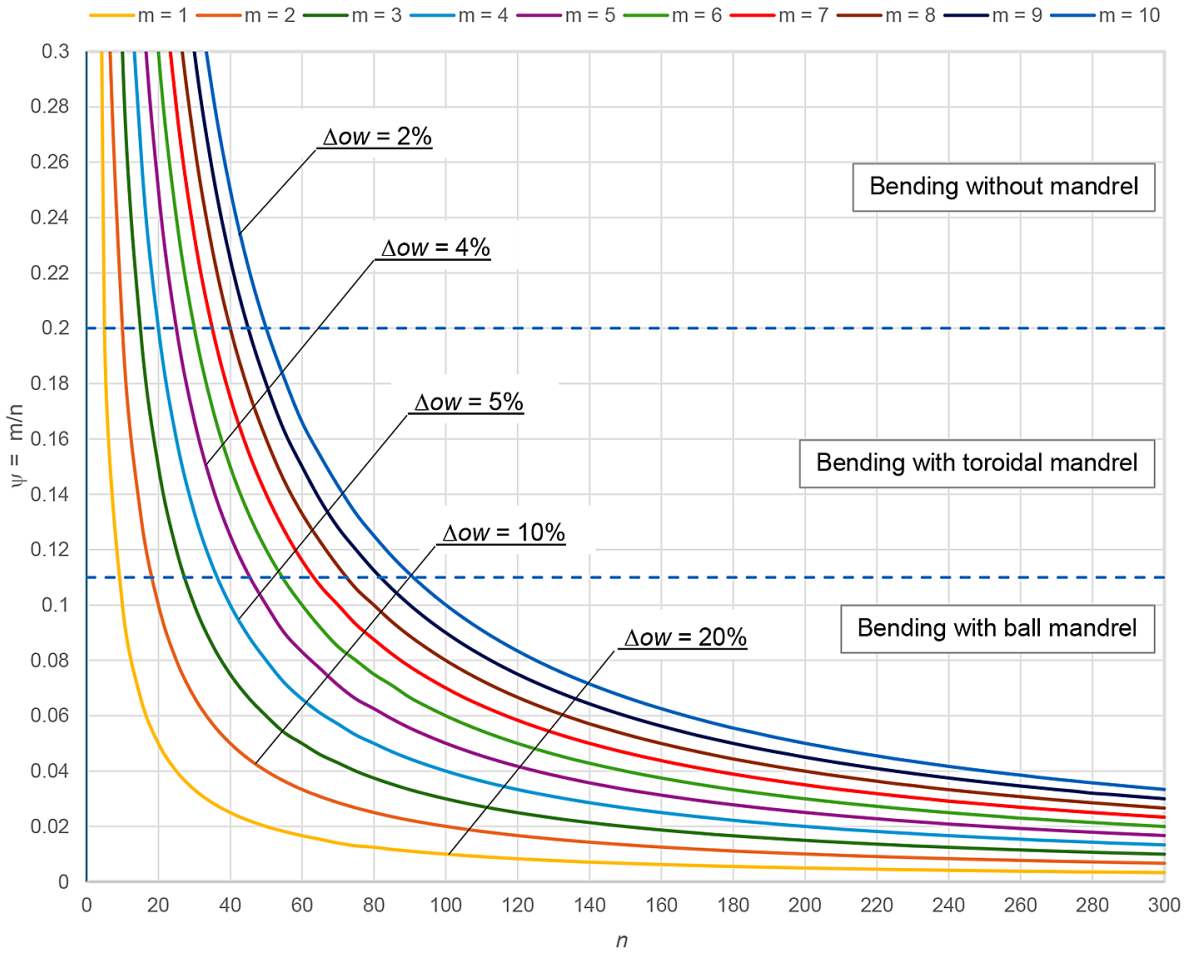

Figure 19. Selection of the bending method depending on the geometrical dimensions and bending radius of the pipe

CONCLUSIONS

The results of the study provide grounds for the conclusion that:

1. Decisive criterion proving the efficiency of the bending process is the acceptable recommended value of ovalisation of the pipe cross-section.
2. Use of a dedicated method of the bending process for the imposed geometric dimensions of the pipe and radius will allow obtaining an ovalisation of the cross-section which does not exceed its acceptable value.
3. Results of the analyses carried out are not only of research importance but also utilitarian, as they enable, on the basis of the nomogram presented in Figure 19, the selection of the bending method for the pipeline bend depending on the dimensions of the pipe cross-section and the bending radius.
4. Use of the proposed toroidal mandrel in the mechanical bending process makes it possible to obtain satisfactory results of the bending process when the value of the ψ coefficient is contained in the range from 0.11 to 0.20.

REFERENCES

1. Bartnik R., Buryn Z., Hnydiuk-Stefan A. Comparative thermodynamic and economic analysis of a conventional gas-steam power plant with a modified gas-steam power plant. Energy Convers. Manag. 2023, 293, 117502.
2. Urbanik M., Tchórzewska-Cieślak B., Pietrucha-Urbanik K. Analysis of the safety of functioning gas pipelines in terms of the occurrence of failures. Energies 2019, 12(17), 3228.
3. Starzyk A., Rybak-Niedziółka K., Łacek P., Mazur Ł., Stefańska A., Kurcjusz M., Nowysz A. Environmental and architectural solutions in the problem of waste incineration plants in Poland: A comparative analysis. Sustainability 2023, 15(3), 2599.
4. Osipowicz T., Koniuszy A., Taustyka V., Abramek

K.F., Mozga Ł. Evaluation of ecological parameters of a compression ignition engine fueled by diesel oil with an Eco Fuel Shot liquid catalyst. Catalyst 2023, 13(12), 1513.

5. Jóźwiak Z. Ships' ballast water in The Southern Baltic area. Sci. J. Marit. Univ. Szczec. 2011, 26(98), 38–46.
6. Młynarczak A. Box coolers as an alternative to existing cooling system. Sci. J. Marit. Univ. Szczec. 2013, 36(108), 131–136.
7. Pavan A.H.V., Vikrant K.S.N., Vimalan G., Singh K. Metallurgical analysis of SA-106 Gr. B pipe failure during hot bending. Case Stud. Eng. Fail. Anal. 2013, 1, 120–130.
8. Szewczyk P. Modern materials and technologies for the construction of high pressure gas pipelines and technological pipelines in mining areas (in Polish). Naft. Gaz 2017, 10, 778–783.
9. Horikawa H., Nobuhisa S. Bending deformation of X80 cold bend pipe. Proceedings of the Nineteenth International Offshore and Polar Engineering Conference, Osaka, Japan, July 21–26, 2009.
10. Sen M., Cheng J.J.R., Zhou J. Behavior of cold bend pipes under bending loads. J. Struct. Eng. 2010, 137(5), 571–578.
11. Naderi G., Torshizi S.E.M., Dibajian S.H. Experimental-numerical study of wrinkling in rotary-draw bending of tight fit pipes. Thin-Walled Struct. 2023, 183, 110428.
12. Fang J., Lu S., Wang K., Xu J., Xu X., Yao Z. Effect of mandrel on cross-section quality in numerical control bending process of stainless steel 2169 small diameter tube. Adv. Mater. Sci. Eng. 2013, 2013, 849495.
13. PN-EN 13480-1, Metallic industrial piping, Part 1: General, Polish Committee for Standardization, Warsaw, Poland, 2024.
14. Płonecki L., Witkowski G., Kurp P. The drives synchronization system for laser-mechanical pipe bending equipment (in Polish). Mechanik 2018, 91(2), 152–154.
15. Traczyk W. Bending of pipes with complex shapes (in Polish). Mag. Przem. 2019, 13(2), 28–31.
16. Packer JA. Bending of hallow structural sections. Available online: https://steeltubeinstitute.Org/resources/hss-bending-hollow-structural-sections/ (accessed on 20 December 2024).
17. Simonetto E., Ghiotti A., Bruschi S. Numerical modelling of direct hot tube rotary draw bending of 22MnB5 high strength steel. CIRP J. Manuf. Sci. Technol. 2022, 37, 547–558.
18. Huang L., Zhang X., Lu X., Zhong Q. Technological parameters optimization and numerical simulation of hot pushing pipe bending process. Int. J. Adv. Manuf. Technol. 2023, 126, 4439–4451.
19. Cheng Z., El-Aty A.A., Zhang R., Cheng C., Guo X., Tao J. Finite element modeling and experimental investigation on manufacturing TA18 alloy pipes via hot free bending forming technology: Forming characteristics and process optimization. J. Mater. Res. Technol. 2024, 29, 5225–5240.
20. Stachowicz F. Bending with upsetting of copper tube elbows. J. Mater. Process Technol. 2000, 100, 236–240.
21. Yang H., Li H., Zhang Z., Zhan M., Liu J., Li G. Advances and trends on tube bending forming technologies. Chin. J. Aeronaut. 2012, 25, 1–12.
22. Moszumański R. Method for bending pipes using a forming block and articulated mandrel for bending pipes, particularly large diameter light-wall tubes. Warsaw, Poland: Polish Patent Office; 2009. Pat.203569, 26.02.2009.
23. Grzegorzewicz J. Tube bending arbour. Warsaw, Poland: Polish Patent Office; 2000. Ru.058109, 4.02.2000.
24. Elyasi M. Effect of the internal pressure in the rubber mandrel on the defects of the rotary draw bending process. J. Mech. Sci. Technol. 2024, 38(3), 1149–1153.
25. Śloderbach Z., Kaźmierczak J. Measurement problems in calculations of the process of bending metal pipes (in Polish). Prz. Mech. 2001, 60(7–8), 38–43.
26. Riagusoff I.I.T., Kenedi P.P., de Souza L.F.G., Pacheco P.M.C.L. Modeling of pipe cold bending: A finite element approach. Proceedings of the VI National Congress of Mechanical Engineering, Campina Granda, Paraiba, Brazil, August 18–21, 2010.
27. Domanowski P., Nowak B. Numerical-experimental analysis of the bending process of tubes made of material with plastic properties (in Polish). Prz. Mech. 2011, 70(6), 23–28.
28. Niezgoda T., Małachowski J., Szymczyk W. Pipelines - numerical modelling and the real state (in Polish). Prz. Mech. 2014, 73(4), 11–18.
29. Sidun P., Łukaszewicz A. Verification of ram-press pipe bending process using elasto-plastic FEM model. Acta Mech. Autom. 2017, 11(1), 47–52.
30. Wang X., Xu J., Ding M., Zhang Y., Wang Z., Guo B., Shan D. Finite-elements modeling and simulation of electrically-assisted rotary-draw bending process for 6063 aluminum alloy micro-tube. Metals 2021, 11(12), 1956.
31. Nozdrzykowski K., Stępień M., Grządziel Z. Assessment of the influence of the bending form shape on the stress and plastic strain values in a cold bending pipe. Sci. J. Marit. Univ. Szczec. 2024, 78(150), 35–48.
32. Wysmulski P. Failure mechanism of tensile CFRP composite plates with variable hole diameter. Materials 2023, 16(13), 4714.
33. Wysmulski P. Numerical and experimental study of crack propagation in the tensile composite plate with the open hole. Adv. Sci. Technol. Res. J. 2023, 17(4), 249–261.

34. Wysmulski P. Analysis of the effect of an open hole on the buckling of a compressed composite plate. Materials 2024, 17(5), 1081.
35. Wang Z., Li J., Liu X., Zhang S., Lin Y., Tan J. Diameter-adjustable mandrel for thin-wall tube bending and its domain knowledge-integrated optimization design framework. Eng. Appl. Artif. Intell. 2025, 139, Part B, 109634.
36. Cheng C., Chen H., Guo J., Guo X., Shi Y. Investigation on the influence of mandrel on the forming quality of thin-walled tube during free bending process. J. Manuf. Process. 2021, 72, 215–226.
37. Jiang L., Lin Y., Li H., Zhang S., Feng Y., Wang Y., Sun M. A new mandrel design with mandrel ball thickness variation for the bending process of aviation ultra-thin-walled tubes. Int. J. Adv. Manuf. Technol. 2022, 122(3–4), 1805–1819.
38. Engel B., Hassan H.R. Investigation of neutral axis shifting in rotary draw bending processes for tubes. Steel Res. Int. 2014, 85(7), 1209–1214.
39. Salem M., Farzin M., Kadkhodaei M., Nakhaei M. A chain link mandrel for rotary draw bending: experimental and finite element study of operation. Int. J. Adv. Manuf. Technol. 2015, 79(5–8), 1071–1080.
40. Razali N.A., Chung S.H., Chung W.J., Joun M.S. Implicit elastoplastic finite element analysis of tube-bending with an emphasis on springback prediction. Int. J. Adv. Manuf. Technol. 2022, 120(9–10), 6377–6391.
41. Nozdrzykowski K., Grządziel Z., Grzejda R., Warzecha M., Stępień M. An analysis of reaction forces in crankshaft support systems. Lubricants 2022, 10(7), 151.
42. Nozdrzykowski K., Grządziel Z., Nozdrzykowska M., Grzejda R., Stępień M. Eliminating the influence of support conditions on geometric shape measurements of large crankshafts of marine engines. Energies 2023, 16(1), 16.
43. Grzejda R. Thermal strength analysis of a steel bolted connection under bolt loss conditions. Eksploat. Niezawodn. – Maint. Reliab. 2022, 24(2), 269–274.
44. Diakun J., Grzejda R. Product design analysis with regard to recycling and selected mechanical properties. Appl. Sci. 2025, 15(2), 512.
45. Grzejda R. The impact of the polymer layer thickness in the foundation shim on the stiffness of the multi-bolted foundation connection. Modelling 2024, 5(4), 1365–1374.
46. PN-EN 13480-1. Metallic industrial piping, Part 1: General. Polish Committee for Standardization: Warsaw, Poland, 2024.
47. PN-EN 12952-3. Water-tube boilers and auxiliary installations, Part 3: Design and calculation for pressure parts of the boiler. Polish Committee for Standardization: Warsaw, Poland, 2023.